Analytica Chimica Acta 1165 (2021) 338549

Contents lists available at ScienceDirect

Analytica Chimica Acta

journal homepage: www.elsevier.com/locate/aca

A novel colorimetric aptasensor for ultrasensitive detection of aflatoxin M_1 based on the combination of CRISPR-Cas12a, rolling circle amplification and catalytic activity of gold nanoparticles

Khalil Abnous [a, b, 1], Noor Mohammad Danesh [b, c, 1], Mohammad Ramezani [a], Mona Alibolandi [a], Morteza Alinezhad Nameghi [a], Taraneh Sadat Zavvar [a], Seyed Mohammad Taghdisi [d, e, *]

[a] Pharmaceutical Research Center, Pharmaceutical Technology Institute, Mashhad University of Medical Sciences, Mashhad, Iran
[b] Department of Medicinal Chemistry, School of Pharmacy, Mashhad University of Medical Sciences, Mashhad, Iran
[c] Research Institute of Sciences and New Technology, Mashhad, Iran
[d] Targeted Drug Delivery Research Center, Pharmaceutical Technology Institute, Mashhad University of Medical Sciences, Mashhad, Iran
[e] Department of Pharmaceutical Biotechnology, School of Pharmacy, Mashhad University of Medical Sciences, Mashhad, Iran

HIGHLIGHTS

- A colorimetric aptasensor is proposed for aflatoxin M_1 (AFM_1) detection.
- It is based on based on the catalytic activity of gold nanoparticles CRISPR-Cas12a and rolling circle amplification.
- This approach is highly sensitive and does not require sophisticated equipment.
- The method achieved a detection limit as low as 0.05 ng/L.
- It could sensitively identify AFM_1 in the spiked milk samples.

ARTICLE INFO

Article history:
Received 10 February 2021
Received in revised form
3 April 2021
Accepted 6 April 2021
Available online 22 April 2021

Keywords:
CRISPR-Cas12a
Colorimetric method
Rolling circle amplification
Gold nanoparticles
Catalytic activity
Ultrasensitive detection

ABSTRACT

Colorimetric approaches have received noticeable attention among sensing methods in view of simplicity and watching the color change of sample by the naked eyes. However, developing colorimetric sensing methods which show high sensitivity is still problematic. Herein, based on CRISPR-Cas12a, rolling circle amplification (RCA) and catalytic activity of gold nanoparticles (AuNPs), a colorimetric aptasensor was introduced for highly sensitive detection of aflatoxin M_1 (AFM_1). In the presence of AFM_1, the CRISPR-Cas12a is inactivated and large single-stranded DNA (ssDNA) structures are formed on the surface of AuNPs following the addition of T4 DNA ligase and phi29 DNA polymerase. So, the sample color remains yellow after addition of 4-nitrophenol. However, no huge DNA structure is observed on the surface of AuNPs in the absence of target because of activation of CRISPR-Cas12a and digestion of primer. So, the color of sample switches to colorless. The results indicated that the biosensor had high selectivity toward AFM_1 and the approach achieved a detection limit as low as 0.05 ng/L. In addition, it could sensitively identify AFM_1 in the spiked milk samples. Overall, this approach is highly sensitive and does not require sophisticated equipment. Therefore, it maintains promising potential for other mycotoxins detection in real samples by simply replacing the applied sequences.

© 2021 Elsevier B.V. All rights reserved.

1. Introduction

Aflatoxins are highly poisonous mycotoxins, generated by *Aspergillus* species [1]. Exposure to these toxic substances leads to unfavorable impacts on human health, including mutagenicity, teratogenicity and carcinogenicity [2].

* Corresponding author. Targeted Drug Delivery Research Center, Pharmaceutical Technology Institute, Mashhad University of Medical Sciences, Mashhad, Iran.
E-mail address: taghdisihm@mums.ac.ir (S.M. Taghdisi).
[1] These authors contributed equally to the work.

https://doi.org/10.1016/j.aca.2021.338549
0003-2670/© 2021 Elsevier B.V. All rights reserved.

Aflatoxins are distributed in a broad range of foodstuffs and agriculture commodities [3]. Aflatoxin M_1 (AFM_1) is the main metabolite of aflatoxin B1 (AFB_1) occurred in milk-based products [4]. This toxin is almost stable through the milk pasteurization procedure [5].

Up to now, numerous techniques have been introduced for quantitative determination of AFM_1, such as enzyme-linked immunosorbent assay (ELISA) [6], high-performance liquid chromatography (HPLC) [7] and thin-layer chromatography [8]. Nevertheless, these approaches demand skilled personnel, costly equipment and laborious pretreatments [9–11]. Thus, introduction of new sensing platforms is desirable for AFM_1 detection.

Aptamers are a class of synthetic nucleic acid molecules that can specifically recognize their target molecules based on steric configuration [12,13]. They are isolated using the Systematic Evolution of Ligands by EXponential enrichment (SELEX), as an *in vitro* technique [14]. Aptamers are regarded as successors of antibodies as a result of their special properties, like reproducible and comfortable synthesis, cost-effective production and extended storage [15,16].

Newly, clustered regularly interspaced short palindromic repeats (CRISPR) has gained wide attentions in different scientific fields, especially in gene editing systems [17]. In this technique, the accuracy of target oligonucleotide cleavage (cis-cleavage) is remarkably promoted since the associated nuclease (Cas) is led through a RNA (crRNA) [18]. Besides cis-cleavage, Cas12a protein can also show a non-selective single-stranded DNA (ssDNA) cleavage (trans-cleavage) [19]. CRISPR-Cas systems own profits, like very high sensitivity and simple fabrication [20]. Using trans-cleavage and the mentioned characteristics, CRISPR-Cas12a has been applied for development of different sensors.

Rolling circle amplification (RCA) is an efficient and simple DNA extension process which can produce long ssDNAs even with length of a few micrometer from short primers in the presence of circular template [21,22]. Recently, this method has been extensively employed in detection systems to enhance the sensitivity [9].

Between the numerous analytical approaches, colorimetric assay has received noticeable attention as a result of its merits, like economical price, plainness and visualized detection [23,24]. Gold nanoparticles (AuNPs) are generally used for construction of colorimetric methods due to their convenient synthesis and modification, distance-dependent surface plasmon resonance, low cost and peroxidase-like activity [25,26].

Based on the mentioned information, herein for the first time, a colorimetric aptasensor was proposed for AFM_1 detection based on the catalytic activity of AuNPs, CRISPR-Cas12a and RCA (Scheme 1). Generally, colorimetric methods show lower sensitivity compared to other approaches like fluorescent or electrochemical-based approaches [27]. In this study, the combination of RCA, CRISPR-Cas12a and AuNPs led to formation of a large DNA structure in the presence of AFM_1 and lack of access of 4-nitrophenol to the surface of AuNPs, while only a very short oligonucleotide remained on the surface of AuNPs when target was absent and 4-nitrophenol freely reached the AuNPs surface, leading to a huge difference between the access of 4-nitrophenol to the AuNPs surface in the absence and presence of AFM_1 and introduction of an ultrasensitive sensing platform for AFM_1 detection which indicates even much better sensitivity in comparison with even electrochemical methods [28].

2. Materials and methods

2.1. Materials

AFM_1 aptamer [29,30] and other sequences were ordered from Microsynth (Switzerland) (Table S1). Ochratoxin A (OTA), tetrachloroauric (III) acid ($HAuCl_4$), aflatoxin M_1 (AFM_1), sodium citrate, sodium borohydride ($NaBH_4$), zearalenone (ZEN), deoxynucleotides (dNTPs), aflatoxin B_1 (AFB_1), 4-nitrophenol, vomitoxin (DON) and tris(2-carboxyethyl) phosphine hydrochloride (TCEP) were obtained from Sigma-Aldrich (USA). T4 DNA ligase and phi29 DNA polymerase were purchased from Thermo Fisher Scientific (USA). EnGen Lba Cas12a (Cpf1) was ordered from New England Biolabs (UK). 10 K centrifugal device was purchased from PALL (USA).

2.2. CRISPR-Cas12a system preparation

400 μL Cas12-crRNA duplex was preassembled in reaction buffer (50 mM NaCl, 10 mM Tris-HCl, 15 mM $MgCl_2$, 1 mM DTT, pH 7.9) containing 200 nM Cas12a and 300 nM crRNA for 30 min at room temperature. To eliminate the unreacted crRNA, the mixture was centrifuged applying 10 K centrifugal device.

2.3. Synthesis of AuNPs

A citrate reduction process was employed to produce AuNPs as mentioned by earlier articles [31]. The shape and size of AuNPs were assessed using transmission electron microscopy (TEM) (CM120, Philips, Netherland) (Fig. S1). The concentration of AuNPs was calculated using extinction coefficient of $2.7 \times 10^8\ M^{-1}\ cm^{-1}$ at $\lambda = 520$ nm.

2.4. Fabrication of primer-modified AuNPs

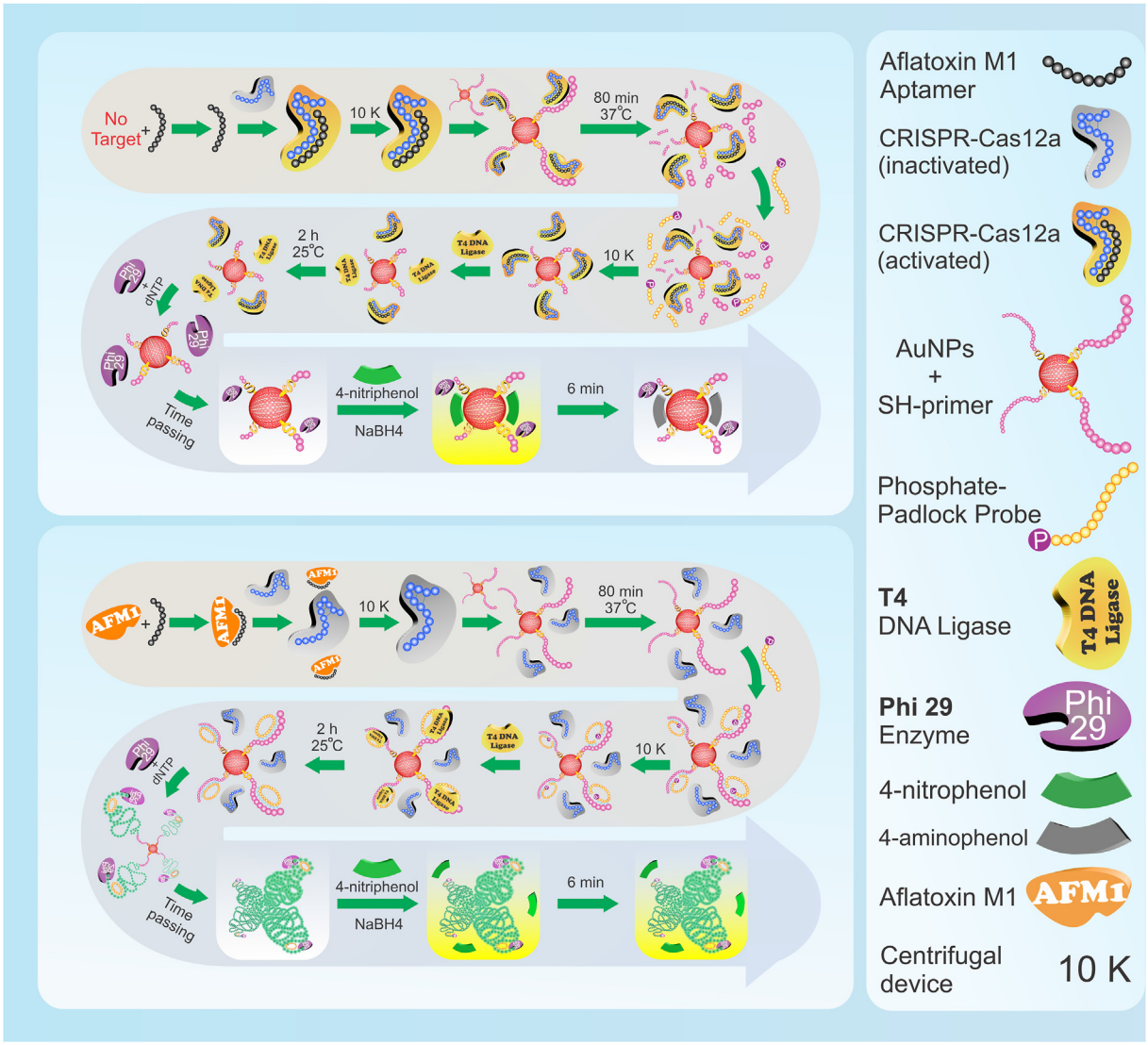
5 mM TCEP was used for pretreatment of thiol-modified primer. 965 μL AuNPs (7 nM) was mixed with 35 μL TCEP-treated primer (8.6 μM) for 12 h at room temperature. The development of primer-modified AuNPs was verified using 3% agarose gel (stained with GelRed).

2.5. Quantification of AFM_1

Firstly, 20 μL AFM_1 aptamer (200 nM) was mixed with 20 μL different concentrations of AFM_1 (0–500 ng/L, dissolved in methanol) and kept 30 min at room temperature. Next, 40 μL of each sample was incubated with 30 μL Cas12a-crRNA duplex (200 nM) for 30 min at room temperature, followed by introductions of 15 μL primer-modified AuNPs (4 nM AuNPs, 170 nM primer) and 55 μL reaction buffer (20 mM NaCl, 4 mM Tris-HCl, 6 mM $MgCl_2$, 0.4 mM DTT, pH 7.9). After 80 min incubation at 37 °C, 2.5 μL padlock probe (1020 nM) was added to each sample and the samples were kept for 1.5 h at room temperature, accompanied by centrifugation using 10 K centrifugal device to remove the unbound and digested padlock probes. In the next step, 20 μL solution containing 1.6× T4 DNA ligase buffer and 12 U T4 DNA ligase was mixed with each sample for 2 h at room temperature. After this, 27 μL solution including 5 mM dNTPs and 1.7× enzyme reaction buffer and 300 U/mL phi29 DNA polymerase was added to the samples and kept at 37 °C for 2 h. Consequently, the samples were mixed with 10 μL 4-nitrophenol (50 mM) and 10 μL $NaBH_4$ (3 M) for 6 min at room temperature, accompanied by measuring the absorbance of each sample (100 μL, diluted 6.6 folds with distilled water) at 400 nM through a Synergy H4 microplate reader (BioTek, USA). It should be considered that the lower concentrations of buffers were used in this section to restrain the aggregation of AuNPs.

2.6. Selectivity evaluation of the biosensor

The specificity of the method was examined by challenging it with diverse toxins, such as AFB_1, DON, OTA, AFM_1 and ZEN. The



Scheme 1. Schematic illustration of colorimetric detection of AFM_1 based on CRISPR-Cas12a, RCA, catalytic activity of AuNPs and aptamer.

quantity of each toxin was 600 ng/L except AFM_1 which was 300 ng/L.

2.7. Milk sample analysis

Milk samples were gathered from a local supermarket. Diverse amounts of AFM_1 (0–500 ng/L) spiked in the milk samples were measured following the protocol in section 2.5. It should be considered that the milk samples were treated with perchloric acid and diluted 20-fold with Tris-HCl (10 mM, pH 7.4).

3. Results and discussion

3.1. Detection strategy of the aptasensor

The steps involved in the fabrication of aptasensor and AFM_1 detection are reviewed in Scheme 1. Lacking of AFM_1, AFM_1 aptamer is hybridized with crRNA and activates CRISPR-Cas12a. Addition of primer-modified AuNPs to the activated CRISPR-Cas12a leads to trans-cleavage and digestion of primer and padlock probe. So, after introduction of padlock probe which has partial complementary regions with primer, no circular template is formed on the surface of AuNPs. In consequence, no long ssDNA is generated on the surface of AuNPs following the addition of T4 DNA ligase and phi29 DNA polymerase. In this case, 4-nitrophenol freely reaches the surface of AuNPs and turned into 4-aminophenol by the peroxidase-mimic activity of AuNPs, causing a color switch from yellow to colorless.

Upon the addition of AFM_1, Aptamer/AFM_1 bioconjugate is shaped and the aptamer cannot bind to crRNA and activate Cas12a. Inactivated CRISPR-Cas12a cannot perform trans-cleavage and degrade primer and so, primer-modified AuNPs remain undamaged. In this case, the both ends of padlock probe can be attached to the primer. So, addition of T4 DNA ligase and phi29 DNA polymerase leads to elongation of 3′-end of primer and production of big DNA structures on the surface of AuNPs (around 500 nm) which can remarkably prevent the entry of 4-nitrophenol to the surface of AuNPs. In this case, the sample color remains yellow.

3.2. Optimization of the colorimetric aptasensor

To improve AFM_1 capture efficiency and maximize the aptasensor response, the detection conditions for AFM_1 were optimized. We noticed the approach presented the best results based

on the following experimental conditions: (a) ratio of 1.5:1 for crRNA to Cas12a in the lack of AFM_1 (Fig. 1A); (b) an incubation time of 80 min for CRISPR-Cas12a to digest primer on the surface of AuNPs and padlock probe in the absence of AFM_1 (Fig. 1B); (c) 1:1 ratio for padlock probe to primer when target was present in the sample (Fig. 1C); (d) a phi29 DNA polymerase concentration of 300 U/mL in the presence of AFM_1 (Fig. 1D); (e) incubation time of 6 min for 4-nitrophenol in the lack of target (Fig. 1E).

3.3. Verification of the aptasensor principle

Gel retardation assay, scanning electron microscope (SEM) and colorimetric measurement were used to survey the assembly and performance of the aptasensor.

Fig. 2 A indicates the electrophoresis image in the presence and absence of AFM_1. Following the immobilization of thiol-labeled primer on the surface of AuNPs, the band of free primer vanished (lane 2), showing the formation of primer-modified AuNPs. After addition of circular template to the primer-modified AuNPs, the band of circular template disappeared (lane 4), suggesting successful hybridization of the both ends of padlock probe with primer. In the case that AFM_1 exists in the sample, a band was observed on the top of gel (lane 5) after addition of T4 DNA ligase and phi29 DNA polymerase, substantiating the efficient elongation of primer and formation of the giant DNA constructions on the surface of AuNPs. While, when the AFM_1 was absent, no band was detectable on the gel (lane 6) after the same treatment. This phenomenon is explained by the activation of CRISPR-Cas12a and digestion of primer and padlock probe in the lack of target. In this case, no attachment happens between digested primer and padlock probe. Consequently, there is no elongation and big DNA structure following treatments with T4 DNA ligase and phi29 DNA polymerase.

The images obtained from SEM corroborated the above mentioned data and showed that in the presence of AFM_1 large DNA structures are formed in the sample which completely hide

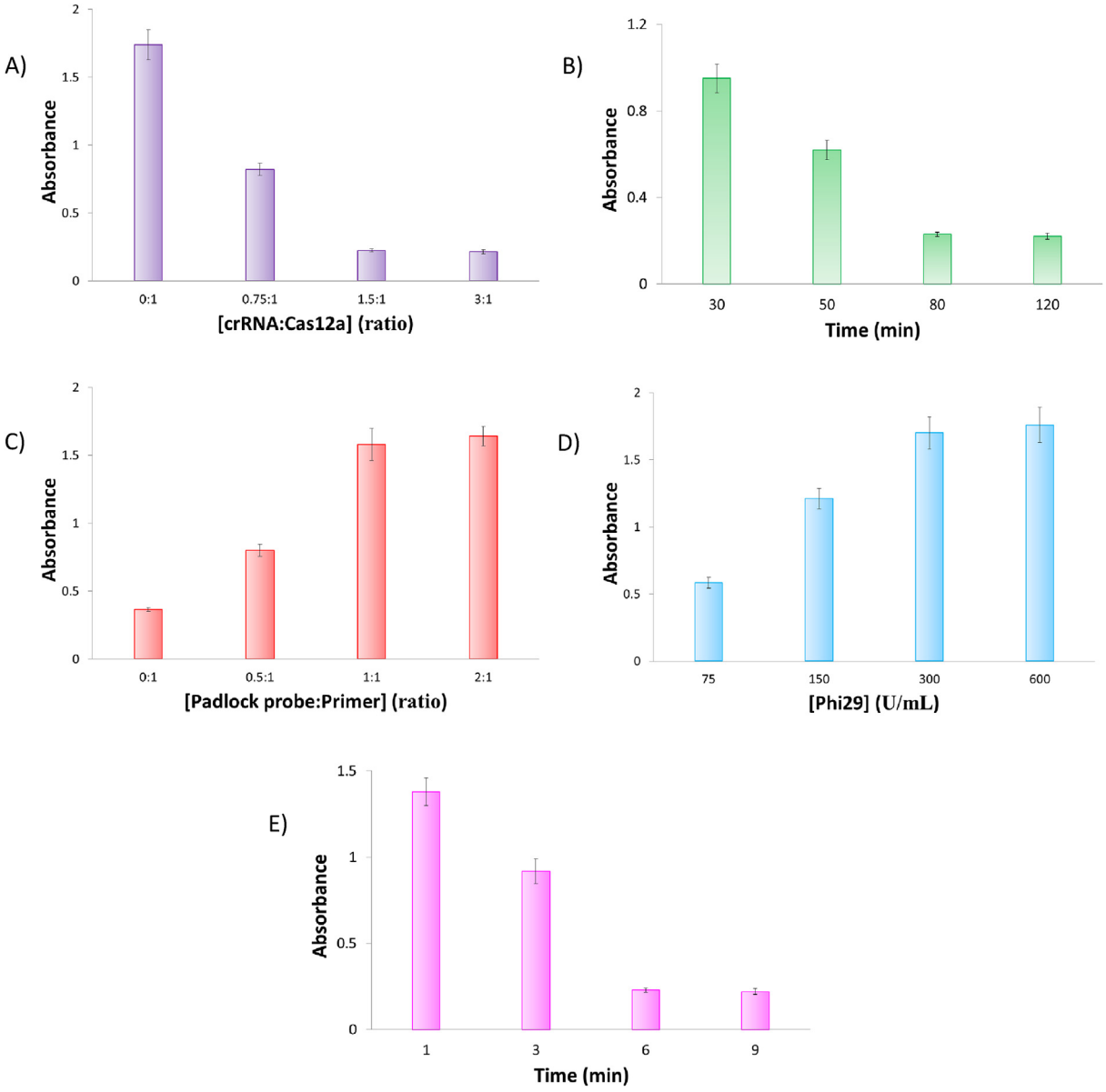


Fig. 1. Optimization of the conditions of aptasensor. (A) Absorbance of the aptasensor at different ratios of crRNA to Cas12a. (B) Absorbance of the method at different incubation times of CRISPR-Cas12a. (C) Absorbance of the approach at various ratios of padlock probe to primer. (D) Absorbance of the approach at diverse concentrations of phi29 DNA polymerase. (E) Absorbance of the sensing method at various incubation times of 4-nitrophenol. The absorbance was measured at 400 nm.

the AuNPs (Fig. 2B). While, in the lack of AFM_1, there is no big DNA construction and AuNPs can be easily detected (Fig. 2C).

To further explore the feasibility of the method, colorimetric measurement was conducted. As illustrated in Fig. 2D, in the blank sample, the sample color changed to colorless and a very faint absorption at 400 nm was detected. It presented that in this situation, the catalytic reaction happened by AuNPs due to the activation of CRISPR-Cas12a and so, lack of formation of large DNA structures around AuNPs. While, the sample color was yellow and a sharp peak was recorded at 400 nm when AFM_1 existed. It indicates that AuNPs have no catalytic activity because their surface has been covered by the large DNA structures and 4-nitrophenol could not reach the surface of AuNPs.

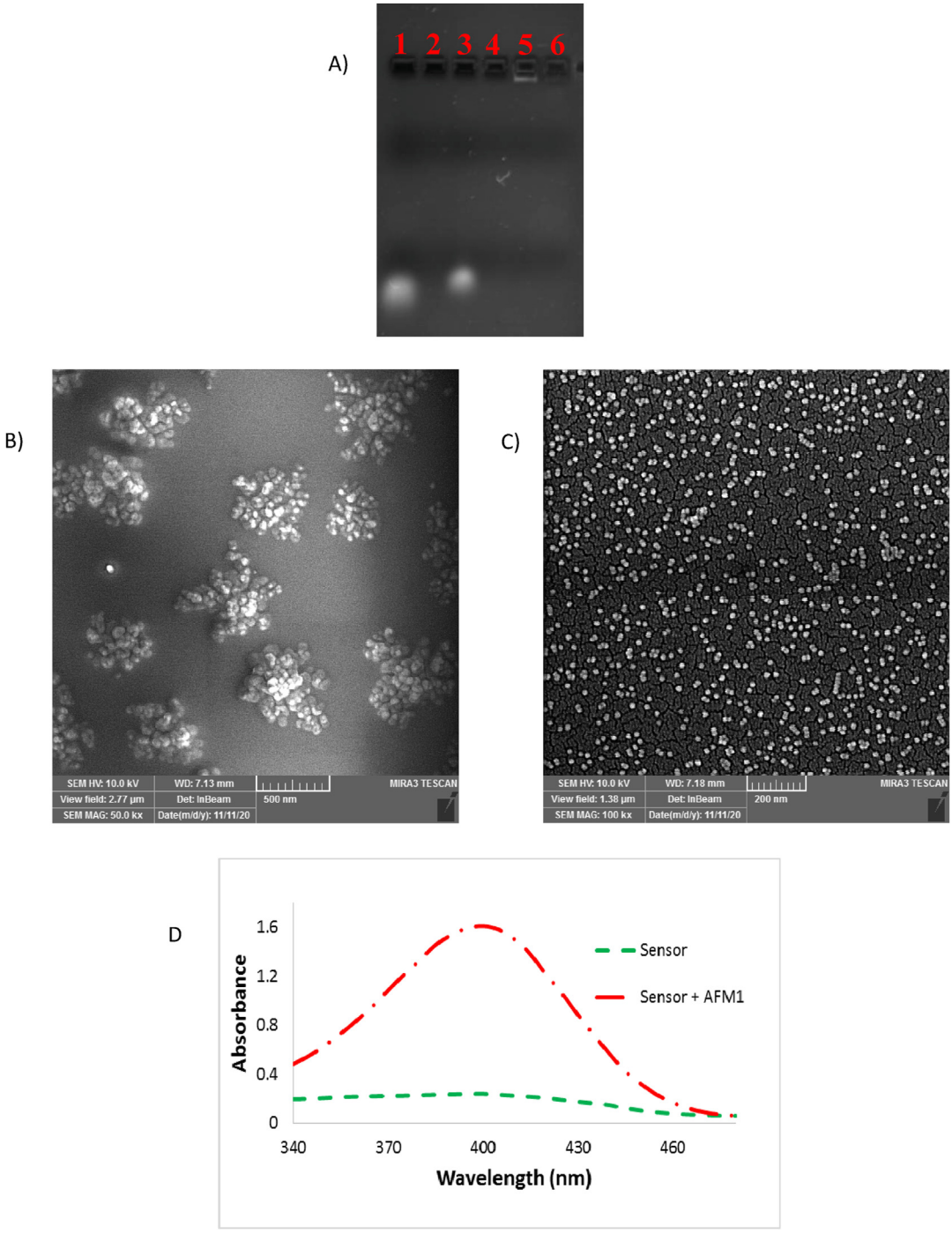


Fig. 2. Analysis of the assembly and performance of the method using gel retardation assay, SEM and colorimetric measurement. (A) Agarose gel electrophoresis (3%, stained with GelRed). Lane 1: free thiol-labeled primer (treated with TCEP), lane 2: thiol-labeled primer + AuNPs (primer-modified AuNPs), lane 3: padlock probe, lane 4: padlock probe + primer-modified AuNPs, lane 5: Sensor + AFM1 (formation of large DNA structures), lane 6: Sensor. SEM images of the sensor in the (B) presence and (C) absence of AFM_1. (D) Absorbance spectra of the sensing strategy in the absence (green curve) and presence of 300 ng/L AFM_1 (red curve). (For interpretation of the references to color in this figure legend, the reader is referred to the Web version of this article.)

3.4. Sensitivity assay for AFM_1

To analyze the capability of the presented method in the quantitative detection of AFM_1, the strategy was used to detect AFM_1 at different concentrations. The color of sample was confirmed to be highly dependent on the concentration of AFM_1 and the sample color changed from colorless to yellow when the amount of target rose (Fig. 3A). The aptasensor showed a wide linear relationship in the range 0.2–300 ng/L AFM_1 (Fig. 3B). The limit of detection (LOD) was calculated to be 0.05 ng/L (S/N = 3). Table 1 compares the presented strategy with previous works for AFM_1 detection [28,29,32–36]. The introduced approach owned better sensitivity than other methods even electrochemical aptasensors.

3.5. Selectivity analysis of the sensing strategy

The colorimetric measurement was applied to examine the selectivity of the analytical strategy to AFM_1 and other toxins, like AFB_1, DON, OTA and ZEN. Fig. 4 exhibited that only the addition of AFM_1 rendered a clear alteration in the relative response of the aptasensor. While, other toxins, even with 2-time higher concentrations, showed very little change in the relative signal of the method, revealing the good specificity of the approach for AFM_1.

3.6. Determination of AFM_1 in milk samples

To examine the functional application of the developed strategy in complex biological samples, the aptasensor was utilized for detection of AFM_1 in the spiked milk samples. The analytical system presented a wide linear relationship in the range of 0.5–350 ng/L with LOD of 0.15 ng/L (S/N = 3) (Fig. S2). This value was lower than the maximum permitted level of AFM_1 in milk introduced by European Commission (50 ng/kg) [37].

The recovery assay was conducted to further test the feasibility of the method in complicated matrices. The recoveries and relative standard deviations (RSDs) were found to be 95–108.23% and 1.38–6.41% (Table S2), respectively that are in good agreements with other analytical approaches. These results corroborated that the designed aptasensor owns high accuracy and reliability.

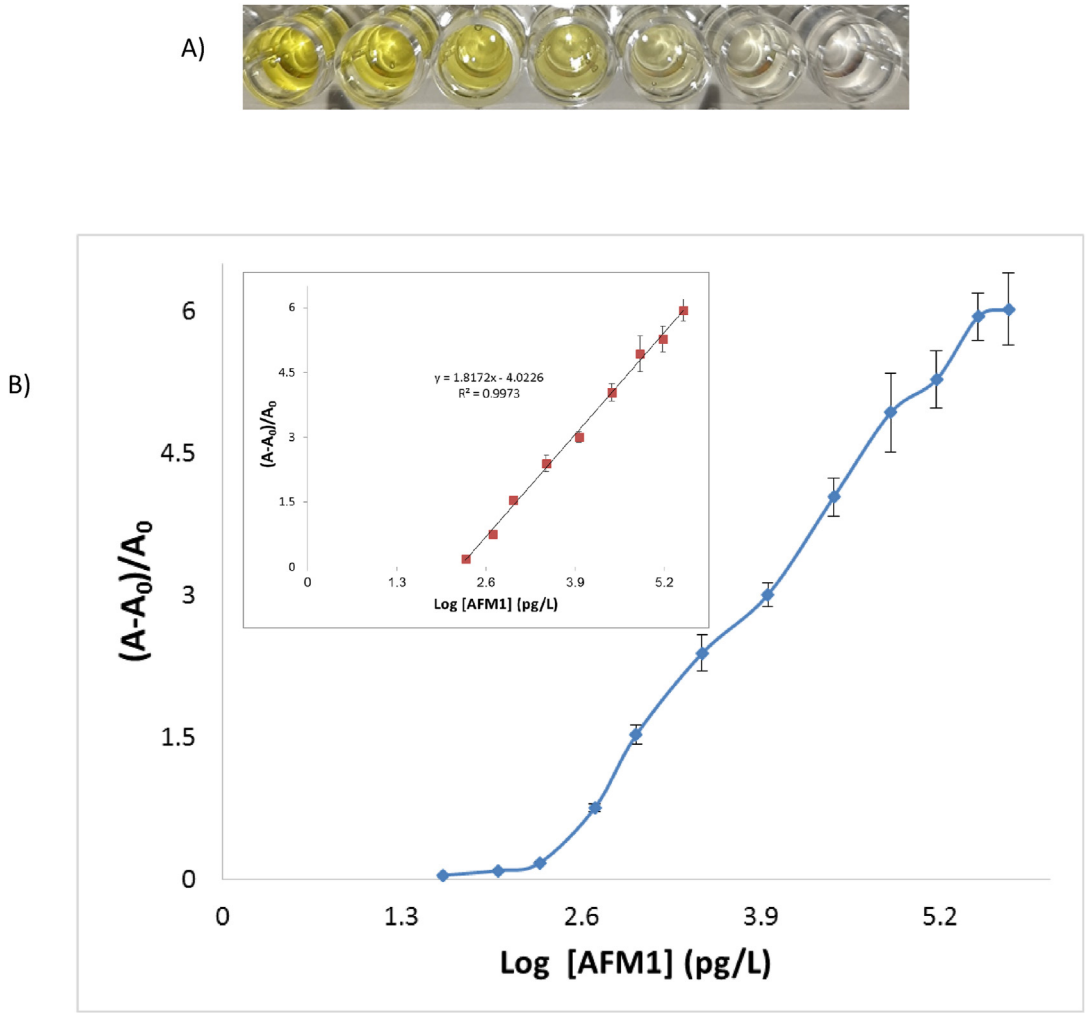


Fig. 3. (A) The color change of samples from colorless to yellow with increasing of the concentration of AFM_1 (0, 0.8, 4, 20, 70, 150 and 300 ng/L of AFM_1 from right to left, respectively). (B) The relative absorbance of the sensing system after treatment with different concentrations of AFM_1 (0–500 ng/L). The inset indicates the linear curve of the relative absorbance. A_0 and A are the absorbance at 400 nm before and after addition of different concentrations of AFM_1, respectively. (For interpretation of the references to color in this figure legend, the reader is referred to the Web version of this article.)

Table 1
Comparison of the presented aptasensor with other reported AFM_1 analytical strategies.

Method	LOD	Linear range	Reference
Rolling circle amplified DNAzyme followed with covalent organic frameworks: Cascade signal amplification of electrochemical ELISA	150 ng/L	500 −80000 ng/L	[32]
Electrochemical Aptasensor with Layer-by-layer Deposited Polyaniline for Voltammetric Determination	1−5 ng/L (Depending on the measurement mode)	3−90 ng/L	[29]
Target-induced DNA machine amplification fluorescence strategy	10 ng/L	10 −2000 ng/L	[33]
Electrochemical Aptasensor Based on Poly(Neutral red)and Carboxylated Pillar [5]arene	0.5 ng/L	5−120 ng/L	[34]
A colorimetric aptasensor based on target-induced protection of gold nanoparticles against salt-induced aggregation and silica nanoparticles	30 ng/L	300 −75000 ng/L	[35]
A electrochemical aptasensor based on target-induced immobilization of gold nanoparticles on the surface of electrode	0.9 ng/L	2−600 ng/L	[28]
Gold nanorods etching-based plasmonic immunoassay	110 ng/L	250 −10000 ng/L	[36]
Our colorimetric aptasensor	0.05 ng/L	0.2−300 ng/L	Current study

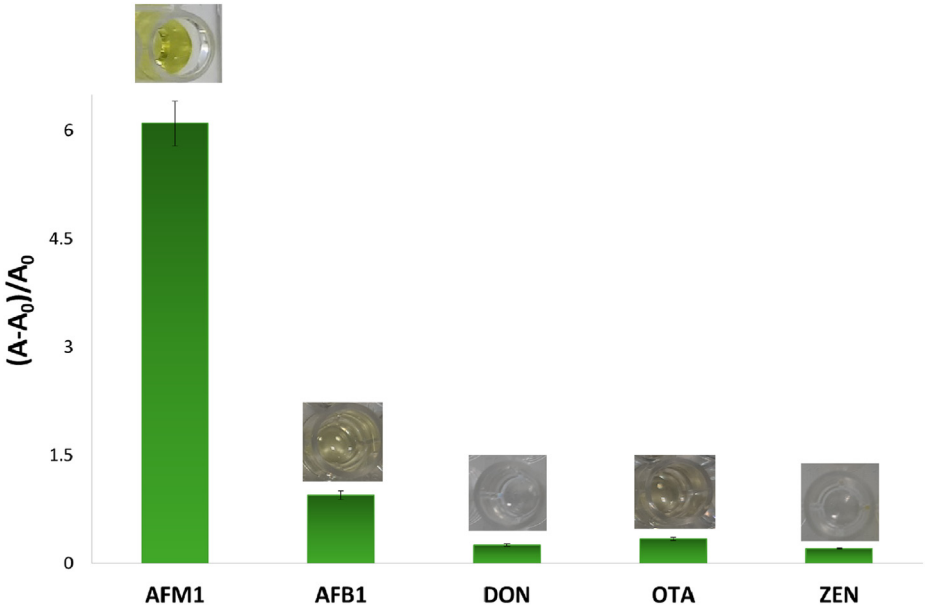


Fig. 4. The relative signal of the sensing method towards AFM_1 and other toxins (the concentration of each toxin was 600 ng/L except AFM_1 which was 300 ng/L). A_0 and A are the absorbance at 400 nm before and after addition of each toxin, respectively.

4. Conclusion

Generally, taking advantages of CRISPR-Cas12a, RCA and catalytic activity of AuNPs, a colorimetric aptasensor was introduced which showed high sensitivity for AFM_1 detection. This colorimetric system achieved the detection range from 0.2 to 300 ng/L with detection limit of 0.05 ng/L. Also, it was revealed that the method owned high selectivity for AFM_1. Furthermore, satisfactory recoveries gained from the spiked milk samples confirmed that the aptasensor can be introduced as an advanced approach for detection of toxins in biological samples.

CRediT authorship contribution statement

Khalil Abnous: Conceptualization, Investigation, Writing − original draft, He has no conflict of interest about this article, All authors have read and approved the final manuscript. **Noor Mohammad Danesh:** Investigation, Writing − original draft, He has no conflict of interest about this article, All authors have read and approved the final manuscript. **Mohammad Ramezani:** Writing − review & editing, Methodology, He has no conflict of interest about this article, All authors have read and approved the final manuscript. **Mona Alibolandi:** Writing − review & editing, Formal analysis, She has no conflict of interest about this article, All authors have read and approved the final manuscript. **Morteza Alinezhad Nameghi:** Visualization, Writing − review & editing, He has no conflict of interest about this article, All authors have read and approved the final manuscript. **Taraneh Sadat Zavvar:** Validation, Writing − review & editing, She has no conflict of interest about this article, All authors have read and approved the final manuscript. **Seyed Mohammad Taghdisi:** Conceptualization, Project administration, Supervision, Funding acquisition, Writing − review & editing, He has no conflict of interest about this article, All authors have read and approved the final manuscript.

Declaration of competing interest

The authors declare that they have no known competing financial interests or personal relationships that could have appeared to influence the work reported in this paper.

Acknowledgment

Financial support of this study was provided by Mashhad University of Medical Sciences.

Appendix A. Supplementary data

Supplementary data to this article can be found online at https://doi.org/10.1016/j.aca.2021.338549.

References

[1] F.N. Ahmad, R. Jamaluddin, N.M. Esa, Screening of the aflatoxin M1 metabolite in urine samples of residents in Terengganu, Malaysia, Toxicon 186 (2020) 120–125.
[2] A. Cherkani-Hassani, I. Ghanname, A. Zinedine, H. Sefrioui, Z. Qmichou, N. Mouane, Aflatoxin M1 prevalence in breast milk in Morocco: associated factors and health risk assessment of newborns "CONTAMILK study,", Toxicon 187 (2020) 203–208.
[3] H. Li, D. Yang, P. Li, Q. Zhang, W. Zhang, X. Ding, J. Mao, J. Wu, Palladium nanoparticles-based fluorescence resonance energy transfer aptasensor for highly sensitive detection of aflatoxin M1 in milk, Toxins 9 (2017).
[4] D. Song, R. Yang, S. Fang, Y. Liu, F. Long, A FRET-based dual-color evanescent wave optical fiber aptasensor for simultaneous fluorometric determination of aflatoxin M1 and ochratoxin A, Microchim. Acta 185 (2018).
[5] A. Sharma, G. Catanante, A. Hayat, G. Istamboulie, I. Ben Rejeb, S. Bhand, J.L. Marty, Development of structure switching aptamer assay for detection of aflatoxin M1 in milk sample, Talanta 158 (2016) 35–41.
[6] S.C. Pei, Y.Y. Zhang, S.A. Eremin, W.J. Lee, Detection of aflatoxin M1 in milk products from China by ELISA using monoclonal antibodies, Food Contr. 20 (2009) 1080–1085.
[7] M. Bognanno, L.L. Fauci, A. Ritieni, A. Tafuri, A. De Lorenzo, P. Micari, L.D. Renzo, S. Ciappellano, V. Sarullo, F. Galvano, Survey of the occurrence of Aflatoxin M1 in ovine milk by HPLC and its confirmation by MS, Mol. Nutr. Food Res. 50 (2006) 300–305.
[8] M. Mwanza, A. Abdel-Hadi, A.M. Ali, M. Egbuta, Evaluation of analytical assays efficiency to detect aflatoxin M1 in milk from selected areas in Egypt and South Africa, J. Dairy Sci. 98 (2015) 6660–6667.
[9] S. Niazi, I.M. Khan, Y. Yu, I. Pasha, Y. Lv, A. Mohsin, B.S. Mushtaq, Z. Wang, A novel fluorescent aptasensor for aflatoxin M1 detection using rolling circle amplification and g-C3N4 as fluorescence quencher, Sensor. Actuator. B Chem. 315 (2020).
[10] H.K. Kordasht, M. Hasanzadeh, Specific monitoring of aflatoxin M1 in real samples using aptamer binding to DNFS based on turn-on method: a novel biosensor, J. Mol. Recogn. 33 (2020).
[11] X. Guo, F. Wen, N. Zheng, S. Li, M.L. Fauconnier, J. Wang, A qPCR aptasensor for sensitive detection of aflatoxin M1, Anal. Bioanal. Chem. 408 (2016) 5577–5584.
[12] S. Wu, Y. Liu, H. Sun, M. Zhong, B. Dai, B. Pan, Z. Shen, An ssDNA aptamer specific for detection and purification of hexahistidine-tagged proteins, Anal. Biochem. 607 (2020).
[13] J. Chen, H. Li, H. Xie, D. Xu, A novel method combining aptamer-Ag10NPs based microfluidic biochip with bright field imaging for detection of KPC-2-expressing bacteria, Anal. Chim. Acta 1132 (2020) 20–27.
[14] Y. He, L. Zhou, L. Deng, Z. Feng, Z. Cao, Y. Yin, An electrochemical impedimetric sensing platform based on a peptide aptamer identified by high-throughput molecular docking for sensitive L-arginine detection, Bioelectrochemistry 137 (2021).
[15] X. Li, P. Zhang, L. Dou, Y. Wang, K. Sun, X. Zhang, G. Song, C. Zhao, K. Li, Y. Bai, X. Zeng, C. Zhou, B. Ying, J. Chen, J. Geng, Detection of circulating tumor cells in breast cancer patients by nanopore sensing with aptamer-mediated amplification, ACS Sens. 5 (2020) 2359–2366.
[16] D. Sun, Y. Wu, S.J. Chang, C.J. Chen, J.T. Liu, Investigation of the recognition interaction between glycated hemoglobin and its aptamer by using surface plasmon resonance, Talanta (2021) 222.
[17] J. Li, S. Yang, C. Zuo, L. Dai, Y. Guo, G. Xie, Applying CRISPR-cas12a as a signal amplifier to construct biosensors for non-DNA targets in ultralow concentrations, ACS Sens. 5 (2020) 970–977.
[18] C.Y. Li, B. Zheng, Y.H. Liu, J.L. Gao, M.Q. Zheng, D.W. Pang, H.W. Tang, A boosting upconversion luminescent resonance energy transfer and biomimetic periodic chip integrated CRISPR/Cas12a biosensor for functional DNA regulated transduction of non-nucleic acid targets, Biosens. Bioelectron. 169 (2020).
[19] H. Li, S. Xing, J. Xu, Y. He, Y. Lai, Y. Wang, G. Zhang, S. Guo, M. Deng, M. Zeng, W. Liu, Aptamer-based CRISPR/Cas12a assay for the ultrasensitive detection of extracellular vesicle proteins, Talanta (2021) 221.
[20] Y. Xiong, J. Zhang, Z. Yang, Q. Mou, Y. Ma, Y. Xiong, Y. Lu, Functional DNA regulated CRISPR-cas12a sensors for point-of-care diagnostics of non-nucleic-acid targets, J. Am. Chem. Soc. 142 (2020) 207–213.
[21] Y. Jiang, Z. Qiu, T. Le, S. Zou, X. Cao, Developing a dual-RCA microfluidic platform for sensitive E. coli O157:H7 whole-cell detections, Anal. Chim. Acta 1127 (2020) 79–88.
[22] S. Xie, J. Zhang, L. Teng, W. Yuan, Y. Tang, Q. Peng, Q. Tang, Electrochemical detection of lipopolysaccharide based on rolling circle amplification assisted formation of copper nanoparticles for enhanced resistance generation, Sensor. Actuator. B Chem. 301 (2019).
[23] J. Qian, C. Ren, C. Wang, K. An, H. Cui, N. Hao, K. Wang, Gold nanoparticles mediated designing of versatile aptasensor for colorimetric/electrochemical dual-channel detection of aflatoxin B1, Biosens. Bioelectron. 166 (2020).
[24] N. Li, S. Zong, Y. Zhang, Z. Wang, Y. Wang, K. Zhu, K. Yang, Z. Wang, B. Chen, Y. Cui, A SERS-colorimetric dual-mode aptasensor for the detection of cancer biomarker MUC1, Anal. Bioanal. Chem. 412 (2020) 5707–5718.
[25] Y. Yang, Y. Yin, X. Li, S. Wang, Y. Dong, Development of a chimeric aptamer and an AuNPs aptasensor for highly sensitive and specific identification of Aflatoxin B1, Sensor. Actuator. B Chem. 319 (2020).
[26] H. Ravan, A. Norouzi, N. Sanadgol, E. Hosseinzadeh, Colorimetric nanoplatform for visual determination of cancer cells via target-catalyzed hairpin assembly actuated aggregation of gold nanoparticles, Mikrochim. Acta 187 (2020) 392.
[27] A. Suea-Ngam, L.-T. Deck, P.D. Howes, A.J. deMello, An ultrasensitive non-noble metal colorimetric assay using starch-iodide complexation for Ochratoxin A detection, Anal. Chim. Acta 1135 (2020) 29–37.
[28] S.H. Jalalian, M. Ramezani, N.M. Danesh, M. Alibolandi, K. Abnous, S.M. Taghdisi, A novel electrochemical aptasensor for detection of aflatoxin M1 based on target-induced immobilization of gold nanoparticles on the surface of electrode, Biosens. Bioelectron. 117 (2018) 487–492.
[29] T.N. Kulikova, A.V. Porfireva, G.A. Evtugyn, T. Hianik, Electrochemical aptasensor with layer-by-layer deposited polyaniline for aflatoxin M1 voltammetric determination, Electroanalysis 31 (2019) 1913–1924.
[30] S. Ben Aissa, A. Mars, G. Catanante, J.L. Marty, N. Raouafi, Design of a redox-active surface for ultrasensitive redox capacitive aptasensing of aflatoxin M1 in milk, Talanta 195 (2019) 525–532.
[31] M. Esmaelpourfarkhani, K. Abnous, S.M. Taghdisi, M. Chamsaz, A novel turn-off fluorescent aptasensor for ampicillin detection based on perylenetetracarboxylic acid diimide and gold nanoparticles, Biosens. Bioelectron. 164 (2020).
[32] Y.H. Pang, L.L. Guo, X.F. Shen, N.C. Yang, C. Yang, Rolling circle amplified DNAzyme followed with covalent organic frameworks: cascade signal amplification of electrochemical ELISA for alfatoxin M1 sensing, Electrochim. Acta 341 (2020).
[33] T. Guo, X. Lin, Y. Liu, J. Deng, P. Qian, Y. Lyu, Z. Zhang, S. Wang, Target-induced DNA machine amplification strategy for high sensitive and selective detection of biotoxin, Sensor. Actuator. B Chem. 262 (2018) 619–624.
[34] V. Smolko, D. Shurpik, A. Porfireva, G. Evtugyn, I. Stoikov, T. Hianik, Electrochemical aptasensor based on poly(neutral red) and carboxylated pillar[5]arene for sensitive determination of aflatoxin M1, Electroanalysis 30 (2018) 486–496.
[35] S.H. Jalalian, P. Lavaee, M. Ramezani, N.M. Danesh, M. Alibolandi, K. Abnous, S.M. Taghdisi, An optical aptasensor for aflatoxin M1 detection based on target-induced protection of gold nanoparticles against salt-induced aggregation and silica nanoparticles, Spectrochim. Acta Mol. Biomol. Spectrosc. 246 (2021) 119062.
[36] B. Fang, S. Xu, Y. Huang, F. Su, Z. Huang, H. Fang, J. Peng, Y. Xiong, W. Lai, Gold nanorods etching-based plasmonic immunoassay for qualitative and quantitative detection of aflatoxin M1 in milk, Food Chem. 329 (2020).
[37] N.S. Shuib, A. Makahleh, S.M. Salhimi, B. Saad, Determination of aflatoxin M1 in milk and dairy products using high performance liquid chromatography-fluorescence with post column photochemical derivatization, J. Chromatogr. A 1510 (2017) 51–56.